Article

Not peer-reviewed version

A Metal Importer and Exporter Interact Differently in the Chloroplast and Cell Membrane

Karnelia Paul , Biswajit Ray , Chinmay Saha , Anupam Roy , Sohini Basu , Anindita Seal *

Posted Date: 17 March 2026

doi: 10.20944/preprints202603.0998.v1

Keywords: *Brassica juncea*; metal homeostasis; *BjYSL6.1; BjYSL6.4; BjNRAMP4.1*

 doi:10.20944/preprints202603.0998.v1

Article

A Metal Importer and Exporter Interact Differently in the Chloroplast and Cell Membrane

Karnelia Paul [1,†], Biswajit Ray [1], Chinmay Saha [1,*], Anupam Roy [1] Sohini Basu [2] and Anindita Seal [1,*]

[1] Department of Biotechnology and Dr. B. C. Guha Centre for Genetic Engineering and Biotechnology, University of Calcutta, 35 Ballygunge Circular Road, Kolkata 700019, India

[2] Department of Biochemistry, University of Calcutta, 35 Ballygunge Circular Road, Kolkata 700019, India

* Correspondence: asbcg@caluniv.ac.in

† Present address: Department of Biology and Howard Hughes Medical Institute, University of North Carolina at Chapel Hill, Chapel Hill, NC, USA.

Abstract

Metal homeostasis, which coordinates the influx and efflux of essential elements such as iron (Fe) and manganese (Mn) in chloroplasts, is essential for optimum photosynthesis, especially in metal-accumulating plants. *Brassica juncea* (Indian mustard) is a metal-tolerant species with a strong metal accumulation capacity, making it a suitable model for studying transition metal homeostasis. In this study, we identified two efflux transporters, *BjYSL6.1* and *BjYSL6.4*, that localize in the endomembrane system of *Schizosaccharomyces pombe* and interact with the chloroplast Mn influx transporter *BjNRAMP4.1* at the plasma membrane and within the chloroplasts. Bimolecular fluorescence complementation and split-ubiquitin yeast two-hybrid assays confirmed specific protein-protein interactions among these transporters, as well as with the membrane-bound thioredoxin *BjHCF164*, a known regulator of photosynthetic electron transport. Gene expression studies revealed that *BjNRAMP4.1* and *BjYSL6* isoforms are inversely regulated under Fe and Mn stress conditions, with *BjNRAMP4.1* being strongly induced under deficiency, whereas *BjYSL6.1* and *BjYSL6.4* are downregulated. These findings suggest that a coordinated network involving *BjNRAMP4.1*, *BjYSL6s*, and *BjHCF164* modulates metal influx and efflux at the chloroplast and plasma membrane interfaces, thereby maintaining metal homeostasis, which is critical for photosynthetic efficiency in *B. juncea*.

Keywords: *Brassica juncea;* metal homeostasis; *BjYSL6.1*; *BjYSL6.4*; *BjNRAMP4.1*

1. Introduction

Yellow stripe-like (YSL) transporters belong to a distinct clade within the oligopeptide transporter (OPT) superfamily. The membrane-bound Fe(III)-phytosiderophore (Fe(III)-PS) transporter of maize, Yellow Stripe 1 (ZmYS1), was the first functionally characterized member of this family [1,2]. The phytosiderophores (PS) are mugineic acid–family compounds secreted by grasses to chelate Fe(III) in the rhizosphere, whereas nicotianamine (NA) is an internal metal chelator that binds Fe(II) and other divalent metals for intracellular and long-distance transport. *ys1* mutant deficient in the maize YS1 protein exhibits interveinal chlorosis or "yellow stripes" due to impaired utilization of Fe(III)-PS complexes [3–6]. The *ZmYS1* gene complements the *fet3fet4* yeast mutant, which is defective in Fe uptake, but only in the presence of Fe(III)-PS [1,7], and electrophysiological studies have confirmed Fe(III)-PS transport activity in Xenopus oocytes [8,9].

Although non-grass species do not synthesize or secrete phytosiderophores, multiple YSL genes have been identified in monocots, dicots, gymnosperms, ferns, and mosses, indicating that these proteins have evolved alternative functions. In these plants, YSLs primarily function as Fe(II)-nicotianamine (Fe(II)-NA) transporters, facilitating long-distance iron translocation and distribution

 doi:10.20944/preprints202603.0998.v1

within the plant, whereas in grasses, YSLs act as (Fe(III)-PS) transporters mediating iron uptake from the rhizosphere [1,10]. In addition to Fe, YSL proteins have been implicated in the transport of other metals, such as Zn, Cu, and Mn [11,12]. Recent genome-wide studies in *Zea mays* and *Nicotiana tabacum* have expanded the known YSL family and revealed diverse expression patterns across tissues and subcellular compartments, reinforcing the multifaceted roles of YSLs in metal uptake, redistribution, and detoxification [10,13].

Metals are continuously trafficked between extracellular spaces and subcellular organelles to maintain metabolic equilibrium [14]. Importantly, while most YSLs have been characterized as metal–nicotianamine importers, YSL4 and YSL6 represent a distinct functional subgroup that operates as metal efflux transporters. Arabidopsis YSL4 and YSL6 localize to the tonoplast and chloroplast envelope, respectively, where they mediate the export of metal-NA complexes from vacuoles or chloroplasts into the cytosol [15,16]. Mutations in *Arabidopsis* YSL4 and YSL6 result in chloroplastic Fe accumulation [16], suggesting that these transporters function as Fe exporters, protecting chloroplasts from metal-induced oxidative damage during germination.

Natural resistance-associated macrophage proteins (NRAMPs) are proton-coupled metal ion transporters that are conserved across prokaryotes and eukaryotes. The first characterized member, NRAMP1, is expressed in mammalian phagosomes during pathogen invasion [17]. In plants, NRAMPs mediate Fe and Mn transport [18–21] and facilitate the movement of other essential and toxic metals, including Zn, Cu, Co, Ni, Cd, Al, and As [22–28].

In *Brassica juncea*, a well-known heavy-metal accumulator, *BjNRAMP4.1*, an ortholog of *AtNRAMP4*, was previously shown to localize not only to the tonoplast, plasma membrane but also to chloroplasts, where it interacts with the thylakoid membrane-bound thioredoxin-like protein *BjHCF164* [29]. The *hcf164* mutant survives only in the heterozygous form and exhibits compromised photosynthesis due to defective redox regulation and cytochrome b6f assembly [30–32]. HCF164 also regulates the kinase STN7/STT7, which modulates short- and long-term photosynthetic acclimation [33,34]. The ability of *BjNRAMP4.1* and *BjHCF164* to interact in both leaf chloroplasts and root membranes suggests that certain transporters may physically associate with redox regulators, potentially linking chloroplast redox balance with metal homeostasis [29].

NRAMP3 and NRAMP4 are critical for mobilizing vacuolar Mn and Fe stores to support chloroplastic photosynthetic demand [20], whereas PAM71 and CMT1 mediate Mn import into the thylakoid lumen and chloroplast stroma, respectively [35–37]. The PIC1 permease functions in Fe import across the chloroplast envelope [38].

In this study, we describe the interaction of *B. juncea* metal transporters *BjYSL6.1* and *BjYSL6.4* with *BjNRAMP4.1* and thioredoxin *BjHCF164*. These interactions occur at both the plasma membrane and chloroplast, suggesting the possibility of coordinated regulation of metal exchange between these compartments during homeostasis. Furthermore, the expression patterns of *BjYSL6.1*, *BjYSL6.4*, and *BjNRAMP4.1* were inversely correlated under Fe and Mn stress, indicating that the opposing regulation of efflux and influx transporters may contribute to maintaining chloroplastic metal homeostasis and redox stability in *Brassica juncea*.

2. Materials and Methods

2.1. Plant Materials and Growth Conditions

B. juncea and *N. benthamiana* seeds (PI 211000) were used for transient expression. The seeds were washed with autoclaved distilled water and placed on wet blotting paper in Petri plates. The plates containing seeds were placed at 4 °C for 24 h for stratification. The next day, they were transferred to a climate-controlled room and incubated for 7 days at 22 °C under a 16 h day (100 µmol $s^{-1}m^{-2}$) and 8 h night cycle at 70% relative humidity. *B. juncea* plants were then transferred to pots and allowed to grow for 15–20 d before infiltration [39]. Six- to 7-week-old *post-germination N. benthamiana plants* were used for agroinfiltration.

 doi:10.20944/preprints202603.0998.v1

2.2. Cloning and Transformation of BjYSL6.1, BjYSL6.4 in Schizosaccharomyces Pombe Vector pDES177N

BjYSL 6.1 and *6.4* were cloned into the entry vector using BP reaction (ThermoFisher Scientific) and sequenced. The constructs were cloned into the *S. pombe* destination vector pDES177N as a fusion of GFP at the N terminus using the LR reaction. S. *pombe* cells were grown in YES medium. For each transformation 0.5-1 mL of cell were used. The cells were centrifuged, and the medium was removed from the cell pellet. Salmon sperm DNA was denatured by heating at 90º C for 5 min and placed on ice to keep it denatured. The cell pellet was resuspended in 0.5 mL PEGLET containing 5 µL salmon sperm DNA and vortexed to mix the solution. The construct (0.5 µg) was added to the destination vector and vortexed to mix. The cells were incubated at 28 °C overnight. The cells were centrifuged the next day, PEGLET was aspirated, 100 µL EMM medium was added, and the entire amount was spread on an EMM (-Uracil) selective plate. The plates were incubated for 3-5 days.

2.3. Confocal Microscopy of GFP: BjYSL6.1-3'UTR and GFP: BjYSL6.4-3'UTR Constructs in S. pombe

GFP: *BjYSL6.1-3*'UTR, GFP: *BjYSL6.4*- 3'UTR, and empty vectors were transformed into *S. pombe.* Cells were inoculated into thiamine-containing minus uracil (-U) synthetic dropout medium and grown to saturation. Cells were washed and inoculated in fresh -U and minus Thiamine (-T) medium for induction of the nmt promoter present in the pDES177N vector at an O.D of 0.2 and then grown until saturation. Cells were stained with HOECSHT (5 µg/mL). The cells were observed under a confocal microscope (Olympus FluoView 1200) using blue excitation (488 nm) and a green emission (509 nm) filter.

2.4. Interaction Between BjYSL6 Proteins with BjNRAMP4.1 and BjHCF164

The entry clone for *BjNRAMP4.1* was mobilized into the pMetYC_GW vector by LR reaction to create bait constructs. *BjNRAMP4.1* was transformed into *Saccharomyces cerevisiae* ThyAP4 cells. ThyAP4 cells containing *BjNRAMP 4.1* were co-transformed with either an empty prey vector (as an autoactivation control) or with *BjYSL6.1* and *BjYSL6.4* in pNXgate32-3HA [40], and transformants were selected on leucine and tryptophan (-L, -W) dropout media. Similarly, to study the interaction between *BjYSL6.1-BjHCF164* and *BjYSL6.4-BjHCF164*, the entry clones for *BjYSL6.1* and *BjYSL6.4* were mobilized into the pMetYC_GW vector to create bait constructs. *BjYSL6.1* and *BjYSL6.4* were transformed into *Saccharomyces cerevisiae* ThyAP4 cells. ThyAP4 cells containing *BjYSL6.1* and *BjYSL6.4* were co-transformed with either an empty prey vector (as an autoactivation control) or with *BjHCF164* cloned in pNXgate32-3HA, and transformants were selected on -L-W media. The positive colonies were grown and spotted on histidine, tryptophan, methionine, and leucine dropout (-H,-W,-M,-L) interaction plates for four days. The agarose overlay assay was performed on yeast patches to select beta-galactosidase-positive colonies. The homodimeric interaction of *the Arabidopsis thaliana* potassium channel protein *KAT1* (AT5G46240) was used as a positive control. ThyAP4 cells transformed with empty bait and prey vectors were used as negative controls.

2.5. β-Galactosidase Assay Using Agarose Overlay

Cells expressing both bait and prey fusions were spotted onto a solid interaction medium. Agarose (0.25 g) was dissolved in 50 mL Z-buffer (60 mM Na_2HPO_4.7 H2O, 40 mM NaH_2PO_4, 10 mM KCl, 1 mM $MgSO_4$.7 H_2O, pH 7.2) with moderate heating in a microwave oven. The agarose solution was cooled to 50 °C in a temperature-controlled water bath. 1 mL of 10% SDS, 0.3 mL β-mercaptoethanol and 1 mL of X-Gal stock solution was added to the Z-buffer agarose mix such that the final concentration of X-Gal was 1 mg/mL. The solution was carefully poured over the plate, and the plate was incubated at 37 °C. The plate was monitored for 15 min to 24 h, depending on the construct.

 doi:10.20944/preprints202603.0998.v1

2.6. Agrobacterium Transformation

Agrobacterium cells (1.5 mL) grown overnight were centrifuged at 14000 rpm for 10 min at 4 °C. The supernatant was discarded, and the pellet was resuspended in 1 mL of ice-cold 20 mM $CaCl_2$ solution. The cells were centrifuged again at 14000 rpm for 5 min at 4 °C, followed by resuspension in 200 µL of ice-cold 20 mM $CaCl_2$. The desired gene was cloned into suitable vectors and used for transformation. Constructs (0.5 – 1 µg) were added to the cell suspension and mixed by pipetting. The microcentrifuge tubes containing the cell suspension were frozen in liquid nitrogen for 5 min, thawed at 37 °C in a water bath for 5 min, and then cooled on ice. YEB medium (1 mL of YEB medium was added to each tube and incubated at 28 °C for 2–5 h with gentle shaking. Finally, 50 – 200 µL of the cells were spread on YEB medium containing appropriate antibiotics and incubated at 28 °C for 2 days. To verify successful transformation, several colonies were randomly selected for plasmid isolation and subjected to PCR using gene-specific primers.

2.7. Localization of BjYSL6.1 and BjYSL6.4 in Brassica Determined by Confocal Microscopy

The BjYSL6.1 and *BjYSL6.4* genes were mobilized into the pMDC45 vector [41,42]. GFP: *BjYSL6.1* and GFP: *BjYSL6.4* were transformed into *Agrobacterium tumefaciens* and selected on YEB plates containing kanamycin (50 µg/mL). *Agrobacterium tumefaciens* grown overnight at 28 °C in YEB medium was diluted to a final $O.D_{600}$ of 0.2 with 10 mM MES-NaOH pH 6.2, 10 mM $MgCl_2$, and acetosyringone (150 µM) and mixed with AvrPto1 (final O.D: 0.1). The AvrPto1 gene was cloned into the pXCSGStrep vector [43] and transformed into *A. tumefaciens* strain GV3101. *B. juncea* cotyledonary leaves were infiltrated as described in Das, Naiya, Marik, Mukherjee and Seal [39] and observed under Confocal laser scanning microscope (Olympus FluoView 1200) 48 h post-infection at an excitation wavelength of 473 nm and emission wavelength of 503-519 nm for GFP.

2.8. Bimolecular Fluorescence Complementation (BiFC) Assay to Study Interaction in Planta

For leaf expression, the plasmids containing the genes of interest were cloned into pSITE-nEYFP-C1 and pSITE-cEYFP-N1 vectors and transformed into *A. tumefaciens* for BiFC studies in plants (*Brassica juncea and Nicotiana benthamiana*). Transformed *A. tumefaciens* (GV3101) was selected on YEB agar plates containing 100 µg/mL of carbenicillin and 50 µg/mL of rifampicin. *A. tumefaciens* expressing *BjYSL6s*, *BjNRAMP4.1* and *BjHCF164* as fusions of the split YFP were grown overnight at 28° C in YEB medium and resuspended in infiltration buffer (10 mM MES-NaOH pH 6.2 and 10 mM $MgCl_2$), acetosyringone (150 µM). The constructs were mixed with *Agrobacterium* cells expressing AvrPto1 (for *B juncea* final O.D. 0.1) [39] or p19 (for *N. benthamiana* final O.D. 1). For transformation in *B. juncea*/*N. benthamiana*, each construct was diluted to a final $O.D_{600}$ of 0.2 and 0.75, respectively. *B. juncea* leaves were infiltrated with mixed cultures of *BjYSL6.1*/*BjYSL6.4* and *BjNRAMP4.1* or *BjYSL6.1*/*BjYSL6.4* and *BjHCF164* along with AvrPto1. The leaves were observed under a confocal microscope 48 h post-infection (hpi). Mixed cultures of *BjNRAMP4.1* and *BjHCF164* were used to infiltrate *B. juncea* leaves and observed under a confocal microscope 72 hpi at an excitation wavelength of 473 nm and emission wavelength of 520-540 nm. *N. benthamiana* leaves were infiltrated with the mixed cultures of *BjYSL6.1*/ *BjYSL6.4* and *BjNRAMP4.1* or *BjYSL6.1*/ *BjYSL6.4* and *BjHCF164* along with p19. Leaves were observed under a confocal microscope 48 hpi. Similarly, mixed cultures of *BjNRAMP4.1* and *BjHCF164* were used to infiltrate *N. benthamiana* leaves and observed under a confocal microscope 72 hpi at an excitation wavelength of 473 nm and emission wavelength of 520-540 nm.

2.9. GUS Staining of Transiently Transformed N. benthamiana Leaves

Nicotiana benthamiana leaves were co-infiltrated with *BjYSL6.1* or *BjYSL6.4* constructs cloned into the pMDC140-GUS vector [41] together with the p19 silencing suppressor. The infiltrated leaves were incubated under standard growth conditions for 48–60 hours post-infiltration. For histochemical analysis, the leaves were vacuum infiltrated with GUS staining buffer as described by Blume and

 doi:10.20944/preprints202603.0998.v1

Grierson [44]. After staining, chlorophyll was removed using 70% ethanol until the tissue became transparent. The samples were then examined under bright-field microscopy using a Nikon Eclipse Ts2R microscope to visualize GUS activity.

2.10. qRT-PCR PCR of BjYSL6 and BjNRAMP4.1 Gene

Total RNA was isolated from the shoots of *B. juncea* plants grown in Murashige and Skoog (MS) medium (control condition), MS medium plus 2 mM Fe and 2 mM Mn (+Fe, +Mn) or MS medium minus Fe or Mn (− Fe, − Mn). Total RNA was isolated from frozen *Brassica* shoot tissues using the HiPurATM Plant and Fungal RNA Miniprep Purification Spin Kit (Himedia, India). RNA was treated with DNase I (1Units/2 µg of RNA) to remove genomic DNA contamination. The integrity of the RNA was checked using formaldehyde agarose gel electrophoresis. To study the expression of metal transporter genes, 5-day old plants grown under +Fe, +Mn, -Fe, and -Mn conditions were compared with untreated controls. RNAs were treated with DNase to remove genomic DNA contamination. A Minus Reverse Transcriptase control was performed with real-time PCR primers (Supplementary Table S1) to check for the removal of contaminating DNA. Primer sequences and PCR conditions are listed in Supplementary Table S1. Single bands of the PCR products for *BjNRAMP4.1, BjYSL6.1, and BjYSL6.4* specific real-time primers showed that the cDNAs were ideal for use in RT-PCR. Two micrograms of total RNA were used to synthesize cDNA with Random Hexamer Primer (Fermentas) using RevertAidTM Reverse Transcriptase (Fermentas 200 units/2 µg of RNA) according to the manufacturer's protocol. The qRT-PCR reaction contained 5 µL DyNAmo ColorFlash SYBR Green I master mix (Thermo Scientific), 0.5 µM of each primer, and 25 ng of cDNA. Real-time PCR was performed using a StepOne Plus real-time PCR machine (Applied Biosystems). The thermal step-up was 10 mins at 95º C, followed by 40 cycles of 10 s at 95º C, 30 s at 65º C. Data analysis was performed using the Expression Suite Software v1.0.4 (Applied Biosystems). Fold change in expression was calculated using the $2^{-\Delta\Delta Ct}$ method and plotted relative to the control using actin as a reference gene via GraphPad Prism 5.02. Experiments were performed in six biological replicates in triplicate. Statistical analysis was performed using Two-way ANOVA followed by Tukey's multiple comparisons test. Statistical significance was set at $P < 0.05$. Different letters indicate significant differences between groups. All data are presented as mean ± SE.

3. Results

3.1. BjYSL6.1 and BjYSL6.4 Are Homologs of Arabidopsis Thaliana YSL6 Protein AtYSL6

BjYSL6.1 and *BjYSL6.4* are two closely related isoforms or allelic variants cloned from the allopolyploid plant *B. juncea*, which are homologs of *AtYSL6* [45]. The two proteins are of equal size and share a high degree of sequence similarity among themselves, with most of the sequence dissimilarities lying in the last exon and 3'UTR (Figure S1). *BjYSL6.1* and *BjNRAMP4.1* were found to interact with (Das and Seal, unpublished data) a chlorophyll-localized tetratricopeptide repeat-containing protein kinase (KM409600, Das, Naiya, Marik, Mukherjee and Seal [39]). As chloroplast localization is found to *AtYSL6* [16], we studied the localization of *BjYSL6.1* and *BjYSL6.4* in plants.

3.2. BjYSL6.1 and BjYSL6.4 Express in the Endomembranes of Schizosaccharomyces Pombe and Shoot Membrane, and Chloroplast of B. juncea

As previous studies have shown that members of the oligopeptide transporter (OPT) family can be mislocalized in *Saccharomyces cerevisiae* [46], we employed *Schizosaccharomyces pombe* (strain GSY001) as a heterologous expression system to investigate the subcellular localization of *BjYSL6.1* and *BjYSL6.4*. The coding sequences of both genes were fused with GFP, and their localization was visualized using confocal microscopy. Cells carrying the empty vector displayed diffuse fluorescence throughout the cytoplasm, indicating a nonspecific distribution of GFP. In contrast, fluorescence from *BjYSL6.1*-GFP and *BjYSL6.4*-GFP was distinctly confined to the plasma membrane and endomembrane system, including the nuclear envelope (Figure 1A; zoomed views). To validate these

 doi:10.20944/preprints202603.0998.v1

observations in planta, *BjYSL6.1*-GFP and *BjYSL6.4*-GFP were transiently expressed in *Brassica juncea* leaves using *Agrobacterium tumefaciens*–mediated infiltration, following a method optimized in our laboratory [39]. Both fusion proteins were predominantly localized to the plasma membrane and chloroplasts, as indicated by the overlap between the GFP and chlorophyll autofluorescence signals (Figure 1B,C).

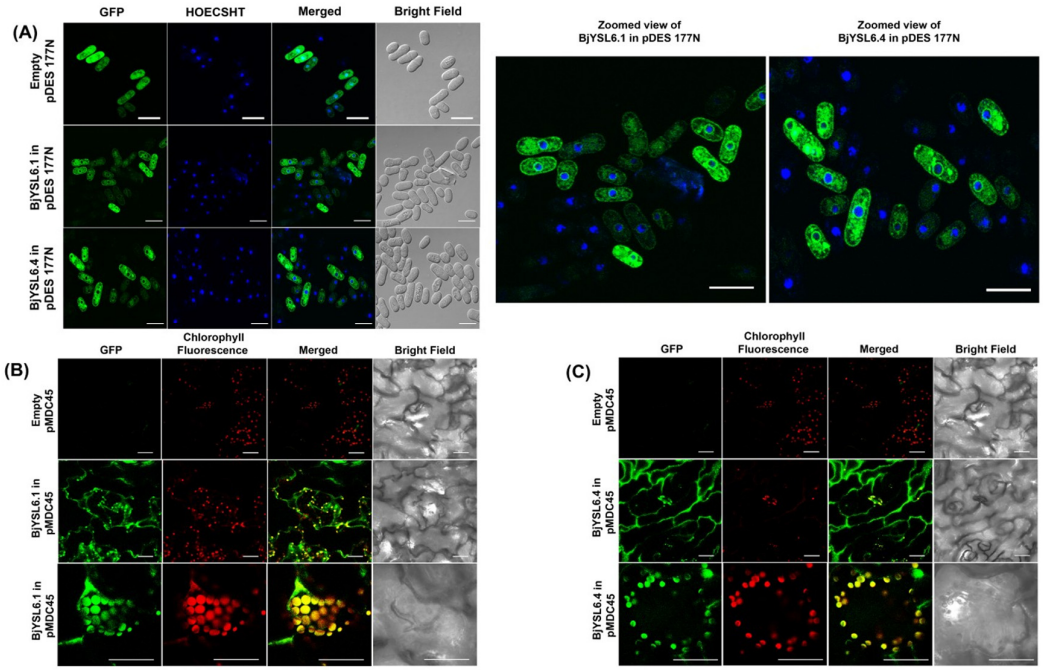

Figure 1. *BjYSL6.1* and *BjYSL6.4* express in the endomembranes of *Schizosaccharomyces pombe* and leaf membrane and chloroplast of *Brassica juncea*. **(A) *BjYSL6.1 and BjYSL6.4 are expressed in the endomembrane of Schizosaccharomyces pombe*.** To study the localization of *BjYSL6.1* and *BjYSL6.4*, the genes were fused to GFP and expressed in *S. pombe* cells. Confocal microscopy was performed. The upper panel shows an empty vector expressed in *S. pombe*. GFP was expressed nonspecifically throughout the cells. *BjYSL6.1* (middle panel) and *BjYSL6.4* (lower panel) fused with GFP expressed at the endomembranes of *S. pombe* (Scale bar: 10 µm). A zoomed version of the middle and lower panels is shown (right) ***(B) BjYSL6.1 and (C) BjYSL6.4 localize to the leaf membrane and chloroplast.*** GFP–*BjYSL6.1* and GFP–*BjYSL6.4* were expressed in *B. juncea* leaves by *A. tumefaciens-mediated* transient expression and imaged using confocal microscopy. (B) Upper panel: Expression of empty pMDC45. Middle panel: GFP–*BjYSL6.1* expressed in the plasma membrane and chloroplast. Lower panel: GFP–*BjYSL6.1* expressed in the chloroplast (Scale bar: 30 µm) (C) Upper panel: empty pMDC45 is expressed. Middle panel GFP–*BjYSL6.4* expresses in the plasma membrane. Lower panel GFP–*BjYSL6.4* expresses in the chloroplast (Scale bar: 30 µm).

3.3. BjYSL6.1 and BjYSL6.4 Exhibit Distinct Interaction Patterns with BjNRAMP4.1 and BjHCF164 in Yeast Two-Hybrid Assays

Previous work using the split-ubiquitin-based yeast two-hybrid (Y2H) system demonstrated that the Mn influx transporter *BjNRAMP4.1* from *Brassica juncea* localizes to the chloroplast and interacts with the membrane-bound thioredoxin *BjHCF164*, a homolog of *Arabidopsis* HCF164 [29]. The Split-Ubiquitin Y2H system is specifically designed to detect interactions involving membrane proteins. In this system, the bait protein is fused to the C-terminal half of ubiquitin (Cub), whereas the prey protein, either cytosolic or membrane-bound, is fused to a mutated N-terminal half of ubiquitin (NubG). Upon bait-prey interaction, the two halves reconstitute functional ubiquitin,

 doi:10.20944/preprints202603.0998.v1

triggering the release of an artificial transcription factor (Protein A-LexA-VP16) that activates reporter genes [47].

To investigate whether *BjYSL6.1* and *BjYSL6.4* interact with *BjNRAMP4.1* and *BjHCF164*, the corresponding genes were cloned into prey vectors and co-transformed with *BjYSL6.1* or *BjYSL6.4* bait constructs into *Saccharomyces cerevisiae* strain THYAP4. Transformed colonies were selected on quadruple dropout (-H,-L,-M,-W) plates and analyzed by spotting and X-gal overlay assays. A strong blue coloration indicated a positive interaction between *BjYSL6.1* and *BjNRAMP4.1*, whereas *BjYSL6.4* showed only a weak interaction (Figure 2A). Similarly, a clear interaction was observed between BjYSL6.1 and BjHCF164, but little or no interaction was detected between *BjYSL6.4* and *BjHCF164* (Figure 2B). Potassium channel KAT1 homodimerization was used as a positive control.

Although *BjYSL6.1* and *BjYSL6.4* share more than 90% amino acid sequence similarity, differing mainly in their final exon and 3′ UTR (Figure S1), their interaction patterns with partner proteins varied markedly. These results suggest that subtle sequence divergence between the two YSL6 isoforms strongly influences their binding specificity in yeast.

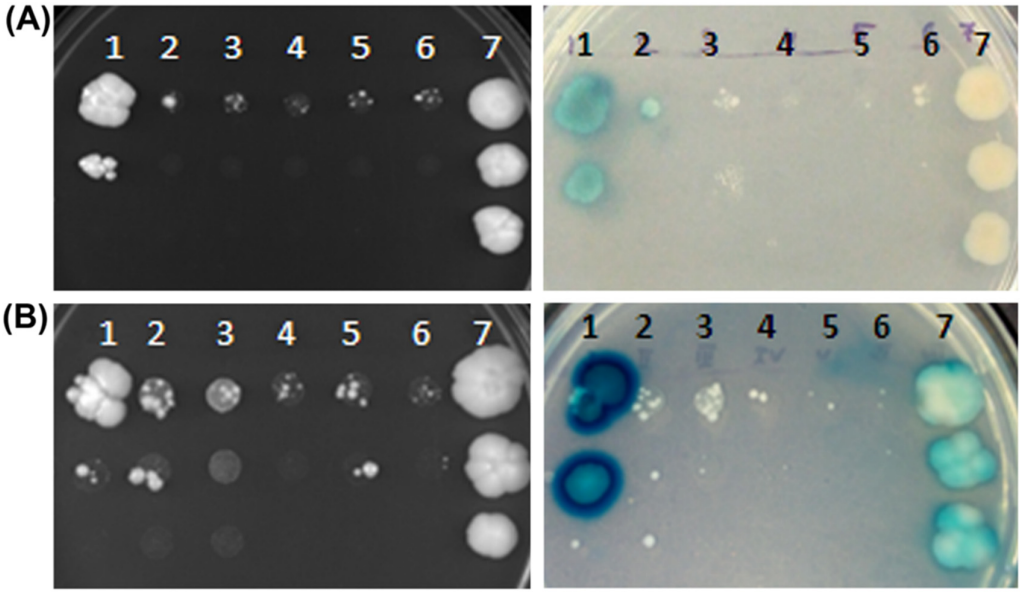

Figure 2. Split Ubiquitin based Yeast Two-hybrid assay shows that both *BjYSL6.1* and *BjYSL6.4* interacts with *BjNRAMP4.1* and *BjHCF164*, but the level of interaction greatly varies depending on its partner protein (A) *BjYSL6.1* or *6.4* and *BjNRAMP4.1* were cotransformed in ThyAP4 yeast cells and selected on interaction (-H-W-M-L) plate. 1. NubG -*BjYSL6.1*- + *BjNRAMP4.1*-Cub, 2. NubG-*BjYSL6.4* + *BjNRAMP4.1*-Cub, 3. Empty pNX32+ *BjNRAMP4.1*-Cub, 4. NubG-*BjYSL6.1* + empty pMetYC, 5. NubG-*BjYSL6.4* + empty pMetYC 6. Empty pNX32+ empty pMetYC, 7. *KAT1*-NubG + *KAT1*-Cub. Left panel: *BjNRAMP4.1* and *BjYSL6.1/6.4* interaction; Right panel: X-Gal overlay assay of *BjNRAMP4.1* and *BjYSL6.1/6.4* interaction. (B) *BjYSL6.1* or *6.4* and *BjHCF164* were co-transformed into ThyAP4 yeast cells and selected on an interaction (-H-W-M-L) plate. 1. *BjYSL6.1*-Cub + NubG-*BjHCF164*, 2. *BjYSL6.4*-Cub + NubG-*BjHCF164*, 3. Empty pMetYC + NubG-*BjHCF164*, 4. *BjYSL6.1*-Cub+ empty pNX32, 5. *BjYSL6.4*-Cub+ empty pNX32, 6. Empty pMetYC + empty pNX32. 7. *KAT1*- NubG + *KAT1*-Cub. Left panel: *BjHCF164* and *BjYSL6.1/6.4* interaction; Right panel: X-Gal overlay assay of *BjHCF164* and *BjYSL6.1/6.4* interaction.

3.4. BjYSL6.1 and BjYSL6.4 Interact with BjNRAMP4.1 and BjHCF164 in Brassica juncea Leaf Albeit Differentially

To examine protein–protein interactions in planta, Bimolecular Fluorescence Complementation (BiFC) assays were performed. The genes were cloned into BiFC vectors pSITE-nEYFP-C1 and pSITE-

 doi:10.20944/preprints202603.0998.v1

cEYFP-N1, and the resulting constructs were co-infiltrated into *Brassica juncea* leaves, as described by Das et al. [39]. Confocal microscopy was performed 48 h post-infiltration to visualize YFP fluorescence as a sign of interaction. Chlorophyll autofluorescence was observed as a chloroplast marker.

BjYSL6.1 and *BjYSL6.4* both interacted with *BjNRAMP4.1*, showing YFP fluorescence at the plasma membrane and in chloroplasts (Figure 3A,B). The co-localization of YFP and chlorophyll fluorescence confirmed chloroplasts as one of the primary sites of interaction. The interactions between *BjYSL6.1*, *BjYSL6.4*, and *BjHCF164* were also analyzed under identical conditions. Both YSL proteins interacted with *BjHCF164*, primarily in chloroplasts (Figure 3C,D). The punctate YFP signals observed at lower magnification (Figure 3C,D, middle panels) largely overlapped with the chlorophyll signal, indicating interaction foci within the chloroplast. No YFP fluorescence was detected in the negative controls, confirming the specificity of the assay. Consistent with our previous observations [29], *BjNRAMP4.1* and *BjHCF164* also interacted at both the plasma membrane and within chloroplasts (Figure 3E).

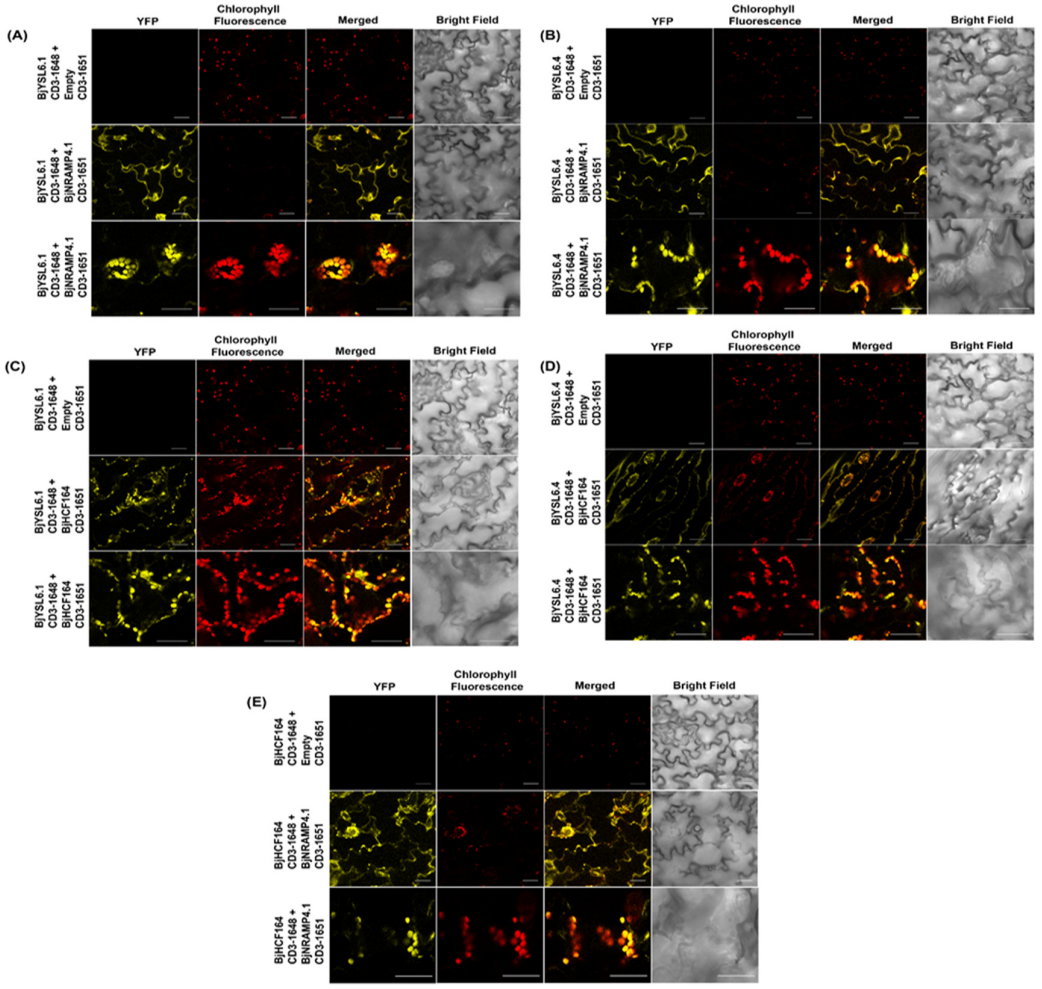

Figure 3. *BjYSL6.1* or *BjYSL6.4* and *BjNRAMP4.1* interact in chloroplast and cell membrane and *BjYSL6.1* or *BjYSL6.4* and *BjHCF164* interact in the chloroplast of *Brassica juncea* leaves. *BjYSL6.1*–nYFP, *BjYSL6.4*-nYFP, and *BjNRAMP4.1*-cYFP were expressed in *Brassica juncea* leaves for the BiFC assay and imaged using confocal microscopy. Chlorophyll fluorescence was used to monitor co-localization in chloroplasts. (A-B) *BjYSL6.1 or BjYSL6.4 and BjNRAMP4.1 interact in the chloroplast.* (A) Upper panel: Leaves transformed with *BjYSL6.*1–nYFP and empty vector -cYFP; Middle panel: *BjYSL6.1*-nYFP and *BjNRAMP4.1*-cYFP interact at the plasma membrane; Lower panel: *BjYSL6.*1-nYFP and *BjNRAMP4.*1-cYFP interact in chloroplasts (Scale bar 30 μm). (B) Upper panel:

 doi:10.20944/preprints202603.0998.v1

Leaves transformed with *BjYSL6.4*–nYFP and empty vector-cYFP; Middle panel: *BjYSL6.4*-nYFP and *BjNRAMP4.1*-cYFP interact at the plasma membrane; Lower panel: *BjYSL6.4*-nYFP and *BjNRAMP4.1*-cYFP interact in chloroplasts (Scale bar 30 µm). (C-D) *BjYSL6.1 or BjYSL6.4 and BjHCF164 interact in the chloroplast.* (C) Upper panel: Leaves transformed with *BjYSL6.1*–nYFP and empty vector-cYFP. Middle panel: *BjYSL6.1*-nYFP and *BjHCF164*-cYFP interact in chloroplast. Lower panel: *BjYSL6.1*-nYFP and *BjHCF164*-cYFP also interacted in chloroplasts (zoomed view, scale bar = 30 µm). (D) Upper panel: Leaves transformed with *BjYSL6.4*–nYFP and empty vector-cYFP; Middle panel: *BjYSL6.4*-nYFP and *BjHCF164*-cYFP interact at the chloroplast. Lower panel: *BjYSL6*.4-nYFP and *BjHCF164*-cYFP also interact in chloroplasts (zoomed view; scale bar = 30 µm). (E) *BjNRAMP4.1 and BjHCF164 interact in the chloroplast and cell membrane of leaves*. *BjHCF164*-nYFP and *BjNRAMP4.1*-cYFP were expressed in *Brassica* leaves for the BiFC assay and imaged using confocal microscopy. Upper panel: Leaves transformed with *BjHCF164*-nYFP and empty vector-cYFP. Middle panel: *BjHCF164*-nYFP and *BjNRAMP4.1*-cYFP interact at the plasma membrane. Lower panel: *BjHCF164*-nYFP and *BjNRAMP4.1*-cYFP interact in chloroplasts (scale bar = 30 µm).

3.5. BjYSL6.1 and BjYSL6.4 Interact with BjNRAMP4.1 and BjHCF164 in Nicotiana benthamiana Leaves

To confirm the protein–protein interactions observed in *Brassica juncea*, we revalidated them in the model plant *Nicotiana benthamiana*. This species is widely used for transient expression assays to analyze subcellular protein localization and protein–protein interactions without requiring stable transformation [48]. For efficient expression in leaves, all constructs were co-infiltrated with the p19 suppressor of post-transcriptional gene silencing (PTGS).

Confocal microscopy was performed 48 h post-infiltration to visualize yellow fluorescent protein (YFP) fluorescence and chlorophyll autofluorescence. Both *BjYSL6.1* and *BjYSL6.4* interacted with *BjNRAMP4.1*, with YFP fluorescence detected at the plasma membrane and within the chloroplasts (Figure 4A,B), consistent with their interaction patterns in *B. juncea*. Overlapping YFP and chlorophyll fluorescence signals confirmed the chloroplast localization of the interaction sites.

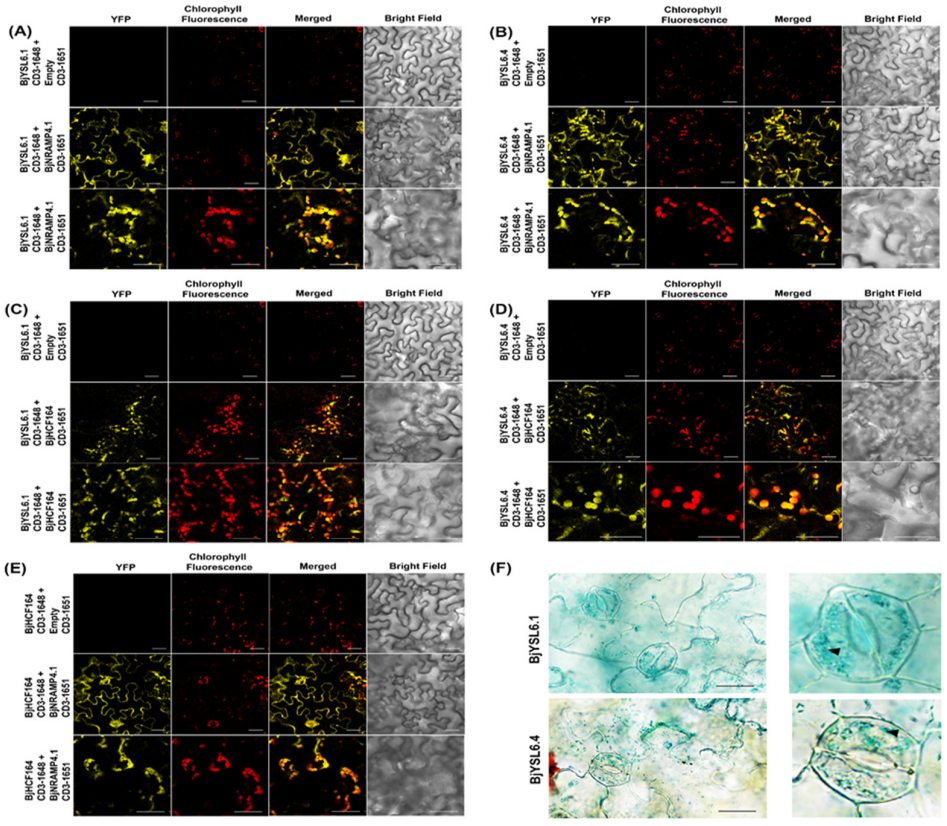

 doi:10.20944/preprints202603.0998.v1

Figure 4. *BjYSL6.1* and *BjYSL6.4* interact with BjNRAMP4.1 in the chloroplast and plasma membrane, and *BjYSL6.1* and *BjYSL6.4* interact with BjHCF164 in the chloroplast of *Nicotiana benthamiana* leaves. *BjYSL6.1*–nYFP, *BjYSL6.4*-nYFP, and *BjNRAMP4.1*-cYFP were expressed in *Nicotiana benthamiana* leaves for BiFC assay and imaged by confocal microscopy. Chlorophyll fluorescence was used to monitor co-localization in chloroplasts. (A-B) ***BjYSL6.1 or BjYSL6.4 and BjNRAMP4.1 interact in the chloroplast.*** (A) Upper panel: Leaves transformed with *BjYSL6.1*–nYFP and empty vector-cYFP; Middle panel: *BjYSL6.1*-nYFP and *BjNRAMP4.1*-cYFP interact at the plasma membrane; Lower panel: *BjYSL6.1*-nYFP and *BjNRAMP4.1*-cYFP interact in chloroplasts (Scale bar 30 μm). (B) Upper panel: Leaves transformed with *BjYSL6.4*–nYFP and empty vector-cYFP; Middle panel: *BjYSL6.4*-nYFP and *BjNRAMP4.1*-cYFP interact at the plasma membrane; Lower panel: *BjYSL6.4*-nYFP and *BjNRAMP4.1*-cYFP interact in chloroplasts (Scale bar 30 μm). (C-D) ***BjYSL6.1 or BjYSL6.4 and BjHCF164 interact in the chloroplast.*** (C) Upper panel: Leaves transformed with *BjYSL6*.1 –nYFP and empty vector-cYFP; middle panel: *BjYSL6.1*-nYFP and *BjHCF164*-cYFP interact in the chloroplast; lower panel: *BjYSL6.1*-nYFP and *BjHCF164*-cYFP also interact in the chloroplasts (zoomed view, scale bar = 30 μm). (D) Upper panel: Leaves transformed with *BjYSL6.4*–nYFP and empty vector-cYFP; Middle panel: *BjYSL6.4*-nYFP and *BjHCF164*-cYFP interact at the chloroplast. Lower panel: *BjYSL6.4*-nYFP and *BjHCF164*-cYFP also interact in chloroplasts (zoomed view; scale bar = 30 μm). (E) ***BjNRAMP4.1 and BjHCF164 interact in the chloroplast and plasma membrane of leaves***. *BjHCF164*-nYFP and *BjNRAMP4.1*-cYFP were expressed in *Nicotiana benthamiana* leaves for the BiFC assay and imaged using confocal microscopy. Upper panel: Leaves transformed with *BjHCF164*-nYFP empty vector-cYFP. Middle panel: *BjHCF164*-nYFP and *BjNRAMP4.1*-cYFP interactions at the plasma membrane; Lower panel: *BjHCF164*-nYFP and *BjNRAMP4.1*-cYFP interactions in chloroplast. (Scale bar 30 μm). (F) ***BjYSL6.1* and *BjYSL6.4* proteins fused with β-glucuronidase (GUS) were expressed in chloroplasts**. *BjYSL6.1* and *BjYSL6.4* proteins were fused to the GUS protein and expressed in *N. benthamiana* leaves. The leaves were infiltrated with GUS staining buffer, destained, and observed under a microscope (scale bar = 10 μm). Arrowheads indicate chloroplasts in the zoomed-in images (right side).

Similarly, interactions between *BjHCF164* and either *BjYSL6.1* or *BjYSL6.4* produced strong YFP fluorescence, which was primarily confined to the chloroplasts (Figure 4C,D). The punctate YFP signals observed at lower magnification largely colocalized with chlorophyll fluorescence, suggesting the presence of interaction foci within the chloroplasts. No fluorescence was detected in the negative controls, confirming the assay specificity.

Consistent with previous reports [29], *BjNRAMP4.1* and *BjHCF164* interacted in both the plasma membrane and chloroplast compartments (Figure 4E). These findings indicate that *BjYSL6* isoforms are associated with distinct chloroplast and membrane partners in a compartment-specific manner.

To further validate chloroplast localization, *BjYSL6.1* and *BjYSL6.4* were fused at their C-termini with the GUS reporter and transiently expressed in *N. benthamiana* leaves. GUS staining revealed blue coloration within the chloroplasts of guard cells, confirming the chloroplast localization of *the BjYSL6.1*-GUS and *BjYSL6.4*-GUS fusion proteins (Figure 4F).

3.6. BjYSL6.1, BjYSL6.4, and BjNRAMP4.1 Exhibit Opposite Transcriptional Expression Under Metal Excess and Deficiency Conditions

Because *BjYSL6* transporters and *BjNRAMP4.1* are involved in Fe and Mn homeostasis, we examined how their expression levels respond to varying metal conditions. Total RNA was isolated from the shoots of *Brassica juncea* plants grown under control conditions (MS medium) or supplemented with 2 mM Fe or 2 mM Mn (+Fe or +Mn). Under excess metal conditions, all three transporters, *BjYSL6.1*, *BjYSL6.4*, and *BjNRAMP4.1*, were downregulated compared to the control. However, the reduction in expression was less pronounced for *BjYSL6.1* and *BjYSL6.4* than for *BjNRAMP4.1*, suggesting a differential transcriptional sensitivity to Fe and Mn excess (Figure 5A).

To further assess their metal-dependent regulation, plants were grown under Fe- or Mn-deficient conditions (− Fe, − Mn). Under these conditions, the expression of *BjNRAMP4.1* was strongly upregulated, whereas *that of BjYSL6.1* and *BjYSL6.4* was downregulated relative to the control (Figure 5B). This inverse regulation pattern indicates that *BjNRAMP4.1* functions predominantly as an influx

 doi:10.20944/preprints202603.0998.v1

transporter activated during Fe or Mn deficiency, whereas *BjYSL6.1* and *BjYSL6.4* likely function as efflux or redistribution transporters that are repressed when external metal availability is low.

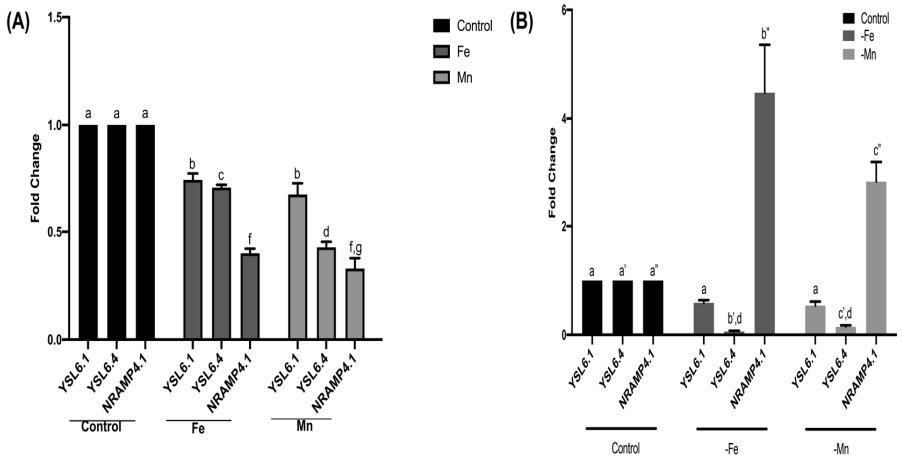

Figure 5. Expression of *BjNRAMP4.1*, *BjYSL6.1* and *BjYSL6.4* in presence of excess and absence of essential metals Expression of YSL and NRAMP was studied using qRT-PCR using RNA from control plants and plants treated with (+Fe, +Mn) or without iron and manganese (− Fe, − Mn). (A) Expression of *BjYSL6.1*, *BjYSL6.4*, and *BjNRAMP4.1* in Fe (2 mM) and Mn (2 mM)-treated plants. (B) Expression of YSL and NRAMP in -Fe and -Mn plants. Statistical analysis was performed using 2-way ANOVA followed by Tukey's multiple comparisons test. Statistical significance was set at $P < 0.05$. Different letters indicate significant differences between groups. All data are presented as mean ± SE.

4. Discussion

Chloroplasts possess a complex internal architecture consisting of a double membrane envelope, stroma where carbon fixation occurs, and thylakoid membrane system that drives photosynthetic electron transport. Proteomic studies have identified more than 90 potential transporters within the chloroplast envelope that supply metal ions and metabolites to sustain chloroplast function [49], although the roles of most remain poorly understood. Oligopeptide and yellow stripe-like (YSL) transporters are associated with distinct functions in long-distance metal circulation, nitrogen assembly, metal sequestration, and glutathione transport, and have been widely implicated in Fe, Zn, and Mn mobilization in plant tissues [10]. The localization of Arabidopsis YSL6 to chloroplasts has been debated since Divol et al. [16] suggested its presence in the chloroplast envelope, although this view remains contested [49]. Mutation in a YSL gene in cucumber *results in a decline in chloroplast-related genes and a* yellow cotyledon phenotype [50].

Here, we demonstrate that two *Brassica juncea* homologs, *BjYSL6.1* and *BjYSL6.4*, share functional similarities with Arabidopsis YSL6 and localize to the chloroplast. Previous work by Divol et al. [16] reported that *AtNRAMP4* protein levels decreased in the *ysl4ysl6* double mutant, implying that *AtYSL4* and *AtYSL6* regulate *AtNRAMP3/4* abundance. Our results are consistent with this relationship, showing that *BjYSL6.1* and *BjYSL6.4* interact with the chloroplastic Mn transporter *BjNRAMP4.1* and membrane-bound thioredoxin *BjHCF164*. In *Schizosaccharomyces pombe, the fluorescence patterns of BjYSL6.1 and BjYSL6.4* suggest localization throughout the endomembrane system, indicating potential trafficking through the secretory pathway.

Chloroplast proteins are generally nuclear-encoded and post-translationally imported via TOC/TIC translocon complexes [51]. However, alternative vesicular routes have been proposed, allowing specific nuclear-encoded proteins to reach chloroplasts independently of the classical import pathways [52]. Our findings that *BjYSL6.1* and *BjYSL6.4* localize to chloroplasts despite

 doi:10.20944/preprints202603.0998.v1

lacking canonical transit peptides suggest that they may use a secretory or vesicle-mediated trafficking route for chloroplast import. Indeed, several plasma membrane and vacuolar proteins, such as Plasma Membrane Intrinsic Proteins (PIPs) and Tonoplast Intrinsic Proteins (TIPs), have been identified in chloroplast proteomes [53,54], indicating that limited inter-organelle trafficking between endomembranes and chloroplasts may not be uncommon.

We previously showed that *BjNRAMP4.1* localizes to the chloroplast and interacts with *BjHCF164*, a thylakoid membrane–bound thioredoxin-like protein [29]. The Arabidopsis ortholog *AtHCF164* is essential for cytochrome b6f complex assembly and mediates redox regulation of the LHCII kinase STN7 via the reduction of luminal cysteine residues. HCF164 integrates short-term state transitions with long-term photosystem stoichiometry adjustments in response to environmental cues. Consistent with these functions, we observed that *BjHCF164*, *BjNRAMP4.1*, and the two *BjYSL6* isoforms localized within chloroplasts and physically interacted. The overlap of GFP and chlorophyll fluorescence signals indicates that these interactions likely occur on the chloroplast envelope and thylakoid membranes, particularly within the stromal thylakoids [55,56].

Iron exporters such as Ferroportins (FPN3/IREG3) play complementary roles in maintaining organellar iron balance in plants. FPN3 functions as a dual-targeted exporter of Fe^{2+} from mitochondria and chloroplasts [57], underscoring that plants employ multiple efflux systems to prevent iron overaccumulation in organelles. The maintenance of organellar homeostasis, such as in chloroplasts, may necessitate the coordinated activity of both importers and exporters. In human functions of DMT1 a NRAMP iron importer protein is regulated by human ferroprotein counterpart [24].

Dual localization of metal transporters is not uncommon, and recent genome-wide analyses of YSL genes in *Nicotiana tabacum* further support their differential expression across tissues and subcellular compartments [13]. Dual expression systems in *B. juncea* and *Nicotiana benthamiana* further support the physiological relevance of these interactions. *N. benthamiana* is well established for high-level transient expression [58], whereas expression in *B. juncea* is lower, reducing the potential artifacts caused by ectopic overexpression. Using the native Brassica system ensured that all four proteins, *BjNRAMP4.1*, *BjYSL6.1*, *BjYSL6.4*, and *BjHCF164*, interacted within their physiological context.

Similar to BjYSL6 transporters, other iron exporters contribute to maintaining organellar iron balance. Notably, the Arabidopsis Ferroportin 3 (FPN3/IREG3) was recently identified as a dual-targeted iron exporter localized to both mitochondria and chloroplasts (Kim et al., 2021). Loss of FPN3 causes iron accumulation in these organelles and triggers increased expression of YSL4/6 and NRAMP4, suggesting a compensatory relationship among iron efflux systems. These findings imply that YSL4/6 and FPN3 share overlapping roles in chloroplast iron export, but differ in substrate specificity. FPN3 exports ferrous ions (Fe^{2+}), whereas YSL4/6 mediate efflux of Fe-nicotianamine complexes. The partial redundancy between these transporters highlights the existence of a coordinated iron efflux network that safeguards chloroplasts and mitochondria from metal-induced oxidative stress.

Recent proteomic analyses of chloroplast envelope fractions by Bouchnak et al. [55] identified *AtHCF164*, *AtYSL6*, and *AtNRAMP4*, among other low-abundance transporters. Despite stringent filtering that excluded *AtYSL6* and *AtNRAMP4* from their final dataset, the detection of all three proteins in their primary screen strongly supports the association of these proteins with chloroplasts. Overly strict bioinformatic cutoffs may exclude transiently or loosely membrane-associated proteins, as evidenced by the absence of the known thylakoid transporter PAM71 in the same dataset. Interestingly, the cyanobacterial homolog *SynPAM71* localizes to both the plasma membrane and thylakoids, mediating Mn export under toxic conditions [59], suggesting that the dual localization of metal transporters may be functionally conserved.

Our results support a model in which *BjNRAMP4.1*, *BjYSL6.1*, *BjYSL6.4*, and *BjHCF164* form a dynamic interaction network bridging the membrane, chloroplast envelope, and thylakoid membranes. Their spatial distribution and expression patterns suggest complementary roles for

 doi:10.20944/preprints202603.0998.v1

BjNRAMP4.1 as an influx transporter, *BjYSL6*s as efflux or redistribution transporters, and *BjHCF164* as a photosynthetic redox regulator. The interplay among these components likely facilitates the fine-tuning of metal homeostasis, redox balance, and photosynthetic efficiency in *B. juncea*.

5. Conclusions

The chloroplast serves as the primary organelle for redox sensing, and both photosynthetic efficiency and chloroplastic redox balance are closely regulated by the availability of Fe and Mn. In this study, we demonstrated that the two yellow stripe-like transporters, *BjYSL6.1* and *BjYSL6.4*, exhibit dual localization similar to the Mn influx transporter *BjNRAMP4.1* and the membrane-bound thioredoxin *BjHCF164*, being present at both the plasma membrane and within chloroplasts. Protein–protein interaction studies revealed that *BjNRAMP4.1*, *BjYSL6.1*, and *BjYSL6.4* interact at both the plasma membrane and chloroplasts, whereas *BjHCF164* interacts primarily with *BjYSL6.1* and *BjYSL6.4* in chloroplasts. These results suggest that these proteins may dynamically associate and potentially shuttle between cellular membranes and chloroplasts in response to metabolic and redox cues. Such interactions likely form an integrated network linking metal homeostasis with photosynthetic regulation, thereby maintaining the optimal balance of essential transition metals within the photosynthetic machinery of *Brassica juncea*.

6. Limitations and Perspectives

In this study, we established the localization and interactions of *BjYSL6.1*, *BjYSL6.4*, *BjNRAMP4.1*, and *BjHCF164* using complementary heterologous and in planta expression systems. Although the data provide strong evidence for their physical association and coordinated transcriptional responses to Fe and Mn status, the precise mechanistic sequence linking these interactions to metal flux and photosynthetic performance remains unclear. The observed dual localization and co-regulation patterns suggest a functional interplay between metal transport and redox regulation; however, further biochemical or physiological studies are required to fully resolve their integrated roles. The present study provides a framework for understanding chloroplast-associated metal transport networks in *Brassica juncea*.

Supplementary Materials: The following supporting information can be downloaded at: Preprints.org.

Acknowledgments: We thank Dr Smrutisanjita Behera CSIR-IICB, Kolkata, West Bengal, India and Dr Senjuti Sinha Roy, NIPGR, New-Delhi, India for *N. benthamiana* seeds. We thank Prof. Wolf B. Frommer for providing the split-ubiquitin two-hybrid system. The pMDC vectors were obtained from ABRC. We thank the Department of Biotechnology-Interdisciplinary Program of Life Sciences for Advanced Research and Education [DBT-IPLS], Calcutta University, for the use of the confocal microscopy facility and Mr. Arijit Pal for his technical assistance in microscopy. The work was funded by the Council of Scientific and Industrial Research (CSIR) [Project No. 38(1276)/10/ EMR-II]. Karnelia Paul's fellowship was provided by the Department of Biotechnology, Government of West Bengal (WBDBT).

Conflicts of Interest: The authors declare no conflicts of interest.

References

1. Curie, C.; Panaviene, Z.; Loulergue, C.; Dellaporta, S.L.; Briat, J.-F.; Walker, E.L. Maize yellow stripe1 encodes a membrane protein directly involved in Fe (III) uptake. *Nature* **2001**, *409*, 346-349, doi:10.1038/35053080.
2. Roberts, L.A.; Pierson, A.J.; Panaviene, Z.; Walker, E.L. Yellow stripe1. Expanded roles for the maize iron-phytosiderophore transporter. *Plant Physiology* **2004**, *135*, 112-120, doi:10.1104/pp.103.037572.
3. Hopkins, B.G.; Jolley, V.D.; Brown, J.C. Plant utilization of iron solubilized by oat phytosiderophore. *Journal of plant nutrition* **1992**, *15*, 1599-1612, doi:10.1080/01904169209364425.

 doi:10.20944/preprints202603.0998.v1

4. Jolley, V.D.; Brown, J.C. Differential response of Fe-efficient corn and Fe-inefficient corn and oat to phytosiderophore released by Fe-efficient Coker 227 oat. *Journal of plant nutrition* **1991**, *14*, 45-58, doi:10.1080/01904169109364182.
5. von Wirén, N.; Marschner, H.; Römheld, V. Uptake kinetics of iron-phytosiderophores in two maize genotypes differing in iron efficiency. *Physiologia Plantarum* **1995**, *93*, 611-616, doi:10.1111/j.1399-3054.1995.tb05107.x.
6. von Wirén, N.; Mori, S.; Marschner, H.; Romheld, V. Iron inefficiency in maize mutant ys1 (Zea mays L. cv Yellow-Stripe) is caused by a defect in uptake of iron phytosiderophores. *Plant Physiology* **1994**, *106*, 71-77, doi:10.1104/pp.106.1.71.
7. Eide, D.; Broderius, M.; Fett, J.; Guerinot, M.L. A novel iron-regulated metal transporter from plants identified by functional expression in yeast. *Proceedings of the National Academy of Sciences of the United States of America* **1996**, *93*, 5624-5628, doi:10.1073/pnas.93.11.5624.
8. Murata, Y.; Ma, J.F.; Yamaji, N.; Ueno, D.; Nomoto, K.; Iwashita, T. A specific transporter for iron (III)–phytosiderophore in barley roots. *The Plant journal* **2006**, *46*, 563-572, doi:10.1111/j.1365-313X.2006.02714.x.
9. Schaaf, G.; Ludewig, U.; Erenoglu, B.E.; Mori, S.; Kitahara, T.; von Wirén, N. ZmYS1 functions as a proton-coupled symporter for phytosiderophore-and nicotianamine-chelated metals. *Journal of Biological Chemistry* **2004**, *279*, 9091-9096, doi:10.1074/jbc.M311799200.
10. Song, Z.; Li, S.; Li, Y.; Zhou, X.; Liu, X.; Yang, W.; Chen, R. Identification and characterization of yellow stripe-like genes in maize suggest their roles in the uptake and transport of zinc and iron. *BMC Plant Biol* **2024**, *24*, 3, doi:10.1186/s12870-023-04691-0.
11. Dai, J.; Wang, N.; Xiong, H.; Qiu, W.; Nakanishi, H.; Kobayashi, T.; Nishizawa, N.K.; Zuo, Y. The Yellow Stripe-Like (YSL) Gene Functions in Internal Copper Transport in Peanut. *Genes (Basel)* **2018**, *9*, doi:10.3390/genes9120635.
12. Kumar, A.; Joon, R.; Singh, G.; Singh, J.; Pandey, A.K. The multifaceted role of YSL proteins: Iron transport and emerging functions in plant metal homeostasis. *Biochim Biophys Acta Gen Subj* **2025**, *1869*, 130792, doi:10.1016/j.bbagen.2025.130792.
13. Yuan, H.; Duan, Z.; Liang, G. Genome-wide identification and expression analysis of yellow stripe-like (YSL) genes in Nicotiana tabacum. *Metallomics* **2025**, *17*, doi:10.1093/mtomcs/mfaf035.
14. Finazzi, G.; Petroutsos, D.; Tomizioli, M.; Flori, S.; Sautron, E.; Villanova, V.; Rolland, N.; Seigneurin-Berny, D. Ions channels/transporters and chloroplast regulation. *Cell Calcium* **2015**, *58*, 86-97, doi:10.1016/j.ceca.2014.10.002.
15. Conte, S.S.; Chu, H.H.; Rodriguez, D.C.; Punshon, T.; Vasques, K.A.; Salt, D.E.; Walker, E.L. Arabidopsis thaliana Yellow Stripe1-Like4 and Yellow Stripe1-Like6 localize to internal cellular membranes and are involved in metal ion homeostasis. *Front Plant Sci* **2013**, *4*, 283, doi:10.3389/fpls.2013.00283.
16. Divol, F.; Couch, D.; Conéjéro, G.; Roschzttardtz, H.; Mari, S.; Curie, C. The Arabidopsis YELLOW STRIPE LIKE4 and 6 Transporters Control Iron Release from the Chloroplast *The Plant Cell* **2013**, *25*, 1040-1055, doi:10.1105/tpc.112.107672.
17. Gruenheid, S.; Pinner, E.; Desjardins, M.; Gros, P. Natural resistance to infection with intracellular pathogens: the Nramp1 protein is recruited to the membrane of the phagosome. *The Journal of experimental medicine* **1997**, *185*, 717-730, doi:10.1084/jem.185.4.717.
18. Cailliatte, R.; Schikora, A.; Briat, J.-F.; Mari, S.; Curie, C. High-affinity manganese uptake by the metal transporter NRAMP1 is essential for Arabidopsis growth in low manganese conditions. *The Plant Cell* **2010**, *22*, 904-917, doi:10.1105/tpc.109.073023.
19. Curie, C.; Alonso, J.M.; Jean, M.L.; Ecker, J.R.; Briat, J.-F. Involvement of NRAMP1 from Arabidopsis thaliana in iron transport. *Biochemical Journal* **2000**, *347*, 749-755, doi:10.1042/bj3470749.
20. Lanquar, V.; Ramos, M.S.; Lelièvre, F.; Barbier-Brygoo, H.; Krieger-Liszkay, A.; Krämer, U.; Thomine, S. Export of vacuolar manganese by AtNRAMP3 and AtNRAMP4 is required for optimal photosynthesis and growth under manganese deficiency. *Plant physiology* **2010**, *152*, 1986-1999, doi:10.1104/pp.109.150946.
21. Yang, M.; Zhang, W.; Dong, H.; Zhang, Y.; Lv, K.; Wang, D.; Lian, X. OsNRAMP3 is a vascular bundles-specific manganese transporter that is responsible for manganese distribution in rice. *PLoS One* **2013**, *8*, e83990, doi:10.1371/journal.pone.0083990.

 doi:10.20944/preprints202603.0998.v1

22. Cailliatte, R.; Lapeyre, B.; Briat, J.-F.; Mari, S.; Curie, C. The NRAMP6 metal transporter contributes to cadmium toxicity. *Biochemical Journal* **2009**, *422*, 217-228, doi:10.1042/BJ20090655.
23. Colangelo, E.P.; Guerinot, M.L. Put the metal to the petal: metal uptake and transport throughout plants. *Current opinion in plant biology* **2006**, *9*, 322-330, doi:10.1016/j.pbi.2006.03.015.
24. Gunshin, H.; Mackenzie, B.; Berger, U.V.; Gunshin, Y.; Romero, M.F.; Boron, W.F.; Nussberger, S.; Gollan, J.L.; Hediger, M.A. Cloning and characterization of a mammalian proton-coupled metal-ion transporter. *Nature* **1997**, *388*, 482-488, doi:10.1038/41343.
25. Nevo, Y.; Nelson, N. The NRAMP family of metal-ion transporters. *Biochimica et Biophysica Acta (BBA)-Molecular Cell Research* **2006**, *1763*, 609-620, doi:10.1016/j.bbamcr.2006.05.007.
26. Sasaki, A.; Yamaji, N.; Yokosho, K.; Ma, J.F. Nramp5 is a major transporter responsible for manganese and cadmium uptake in rice. *The Plant Cell* **2012**, *24*, 2155-2167, doi:10.1105/tpc.112.096925.
27. Tiwari, M.; Sharma, D.; Dwivedi, S.; Singh, M.; Tripathi, R.D.; Trivedi, P.K. Expression in A rabidopsis and cellular localization reveal involvement of rice NRAMP, OsNRAMP 1, in arsenic transport and tolerance. *Plant, Cell & Environment* **2014**, *37*, 140-152, doi:10.1111/pce.12138.
28. Xia, J.; Yamaji, N.; Kasai, T.; Ma, J.F. Plasma membrane-localized transporter for aluminum in rice. *Proceedings of the National Academy of Sciences* **2010**, *107*, 18381-18385, doi:10.1073/pnas.1004949107.
29. Marik, A.; Naiya, H.; Das, M.; Mukherjee, G.; Basu, S.; Saha, C.; Chowdhury, R.; Bhattacharyya, K.; Seal, A. Split-ubiquitin yeast two-hybrid interaction reveals a novel interaction between a natural resistance associated macrophage protein and a membrane bound thioredoxin in Brassica juncea. *Plant molecular biology* **2016**, *92*, 519-537, doi:10.1007/s11103-016-0528-x.
30. Gabilly, S.T.; Dreyfuss, B.W.; Karamoko, M.; Corvest, V.; Kropat, J.; Page, M.D.; Merchant, S.S.; Hamel, P.P. CCS5, a thioredoxin-like protein involved in the assembly of plastid c-type cytochromes. *Journal of Biological Chemistry* **2010**, *285*, 29738-29749, doi:10.1074/jbc.M109.099069.
31. Lennartz, K.; Plücken, H.; Seidler, A.; Westhoff, P.; Bechtold, N.; Meierhoff, K. HCF164 encodes a thioredoxin-like protein involved in the biogenesis of the cytochrome b6f complex in Arabidopsis. *The Plant Cell* **2001**, *13*, 2539-2551, doi:10.1105/tpc.010245.
32. Motohashi, K.; Hisabori, T. HCF164 receives reducing equivalents from stromal thioredoxin across the thylakoid membrane and mediates reduction of target proteins in the thylakoid lumen. *The Journal of biological chemistry* **2006**, *281*, 35039-35047, doi:10.1074/jbc.M605938200.
33. Lemeille, S.; Willig, A.; Depège-Fargeix, N.; Delessert, C.; Bassi, R.; Rochaix, J.-D. Analysis of the chloroplast protein kinase Stt7 during state transitions. *PLoS Biol* **2009**, *7*, e1000045, doi:10.1371/journal.pbio.1000045.
34. Pesaresi, P.; Hertle, A.; Pribil, M.; Kleine, T.; Wagner, R.; Strissel, H.; Ihnatowicz, A.; Bonardi, V.; Scharfenberg, M.; Schneider, A. Arabidopsis STN7 kinase provides a link between short-and long-term photosynthetic acclimation. *The Plant Cell* **2009**, *21*, 2402-2423, doi:10.1105/tpc.108.064964.
35. Eisenhut, M.; Hoecker, N.; Schmidt, S.B.; Basgaran, R.M.; Flachbart, S.; Jahns, P.; Eser, T.; Geimer, S.; Husted, S.; Weber, A.P.M.; et al. The Plastid Envelope CHLOROPLAST MANGANESE TRANSPORTER1 Is Essential for Manganese Homeostasis in Arabidopsis. *Molecular Plant* **2018**, *11*, 955-969, doi:10.1016/j.molp.2018.04.008.
36. Schneider, A.; Steinberger, I.; Herdean, A.; Gandini, C.; Eisenhut, M.; Kurz, S.; Morper, A.; Hoecker, N.; Rühle, T.; Labs, M.; et al. The evolutionarily conserved protein PHOTOSYNTHESIS AFFECTED MUTANT71 is required for efficient manganese uptake at the thylakoid membrane in Arabidopsis. *The Plant Cell* **2016**, *28*, tpc.00812.02015, doi:10.1105/tpc.15.00812.
37. Zhang, B.; Zhang, C.; Liu, C.; Jing, Y.; Wang, Y.; Jin, L.; Yang, L.; Fu, A.; Shi, J.; Zhao, F.; et al. Inner Envelope CHLOROPLAST MANGANESE TRANSPORTER 1 Supports Manganese Homeostasis and Phototrophic Growth in Arabidopsis. *Molecular Plant* **2018**, *11*, 943-954, doi:10.1016/j.molp.2018.04.007.
38. Duy, D.; Stübe, R.; Wanner, G.; Philippar, K. The Chloroplast Permease PIC1 Regulates Plant Growth and Development by Directing Homeostasis and Transport of Iron *Plant Physiology* **2011**, *155*, 1709-1722, doi:10.1104/pp.110.170233.
39. Das, M.; Naiya, H.; Marik, A.; Mukherjee, G.; Seal, A. A protocol for functional study of genes in Brassica juncea by Agrobacterium-mediated transient expression: applicability in other Brassicaceae. *Journal of Plant Biochemistry and Biotechnology* **2020**, *29*, 368-379, doi:10.1007/s13562-019-00543-x.

 doi:10.20944/preprints202603.0998.v1

40. Lalonde, S.; Sero, A.; Pratelli, R.; Pilot, G.; Chen, J.; Sardi, M.I.; Parsa, S.A.; Kim, D.Y.; Acharya, B.R.; Stein, E.V.; et al. A membrane protein/signaling protein interaction network for Arabidopsis version AMPv2. *Frontiers in physiology* **2010**, *1*, 24, doi:10.3389/fphys.2010.00024.
41. Curtis, M.D.; Grossniklaus, U. A gateway cloning vector set for high-throughput functional analysis of genes in planta. *Plant physiology* **2003**, *133*, 462-469, doi:10.1104/pp.103.027979.
42. Xu, R.; Qingshun, L.Q. Protocol: Streamline cloning of genes into binary vectors in Agrobacterium via the Gateway® TOPO vector system. *Plant Methods* **2008**, *4*, 4, doi:10.1186/1746-4811-4-4.
43. Noël, L.D.; Cagna, G.; Stuttmann, J.; Wirthmüller, L.; Betsuyaku, S.; Witte, C.-P.; Bhat, R.; Pochon, N.; Colby, T.; Parker, J.E. Interaction between SGT1 and Cytosolic/Nuclear HSC70 Chaperones Regulates Arabidopsis Immune Responses. *The Plant Cell* **2007**, *19*, 4061-4076, doi:10.1105/tpc.107.051896.
44. Blume, B.; Grierson, D. Expression of ACC oxidase promoter-GUS fusions in tomato and Nicotiana plumbaginifolia regulated by developmental and environmental stimuli. *Plant J* **1997**, *12*, 731-746, doi:10.1046/j.1365-313x.1997.12040731.x.
45. Das, S.; Sen, M.; Saha, C.; Chakraborty, D.; Das, A.; Banerjee, M.; Seal, A. Isolation and expression analysis of partial sequences of heavy metal transporters from Brassica juncea by coupling high throughput cloning with a molecular fingerprinting technique. *Planta* **2011**, *234*, 139-156, doi:10.1007/s00425-011-1376-1.
46. Thakur, A.; Bachhawat, A.K. Mutations in the N-terminal region of the Schizosaccharomyces pombe glutathione transporter pgt1+ allows functional expression in Saccharomyces cerevisiae. *Yeast* **2013**, *30*, 45-54, doi:10.1002/yea.2939.
47. Thaminy, S.; Miller, J.; Stagljar, I. The Split-Ubiquitin Membrane-Based Yeast Two-Hybrid System. *Methods in molecular biology (Clifton, N.J.)* **2004**, *261*, 297-312, doi:10.1385/1-59259-762-9:297.
48. Sparkes, I.A.; Runions, J.; Kearns, A.; Hawes, C. Rapid, transient expression of fluorescent fusion proteins in tobacco plants and generation of stably transformed plants. *Nat Protoc* **2006**, *1*, 2019-2025, doi:10.1038/nprot.2006.286.
49. Schmidt, S.B.; Eisenhut, M.; Schneider, A. Chloroplast Transition Metal Regulation for Efficient Photosynthesis. *Trends in Plant Science* **2020**, *25*, 817-828, doi:10.1016/j.tplants.2020.03.003.
50. Pan, J.; Song, J.; Sharif, R.; Xu, X.; Li, S.; Chen, X. A mutation in the promoter of the yellow stripe-like transporter gene in cucumber results in a yellow cotyledon phenotype. *Journal of Integrative Agriculture* **2024**, *23*, 849-862, doi:10.1016/j.jia.2023.11.024.
51. Blum, H.; Beier, H.; Gross, H.J. Improved silver staining of plant proteins, RNA and DNA in polyacrylamide gels. *Electrophoresis* **1987**, *8*, 93-99, doi:10.1002/elps.1150080203.
52. Villarejo, A.; Burén, S.; Larsson, S.; Déjardin, A.; Monné, M.; Rudhe, C.; Karlsson, J.; Jansson, S.; Lerouge, P.; Rolland, N.; et al. Evidence for a protein transported through the secretory pathway en route to the higher plant chloroplast. *Nature cell biology* **2005**, *7*, 1224-1231, doi:10.1038/ncb1330.
53. Daher, Z.; Recorbet, G.; Valot, B.; Robert, F.; Balliau, T.; Potin, S.; Schoefs, B.; Dumas-Gaudot, E. Proteomic analysis of Medicago truncatula root plastids. *Proteomics* **2010**, *10*, 2123-2137, doi:10.1002/pmic.200900345.
54. Ferro, M.; Brugière, S.; Salvi, D.; Seigneurin-Berny, D.; Court, M.; Moyet, L.; Ramus, C.; Miras, S.; Mellal, M.; Le Gall, S.; et al. AT_CHLORO, a comprehensive chloroplast proteome database with subplastidial localization and curated information on envelope proteins. *Mol Cell Proteomics* **2010**, *9*, 1063-1084, doi:10.1074/mcp.M900325-MCP200.
55. Bouchnak, I.; Brugière, S.; Moyet, L.; Le Gall, S.; Salvi, D.; Kuntz, M.; Tardif, M.; Rolland, N. Unraveling Hidden Components of the Chloroplast Envelope Proteome: Opportunities and Limits of Better MS Sensitivity*[S]. *Molecular & Cellular Proteomics* **2019**, *18*, 1285-1306, doi:10.1074/mcp.RA118.000988.
56. Duan, Z.; Kong, F.; Zhang, L.; Li, W.; Zhang, J.; Peng, L. A bestrophin-like protein modulates the proton motive force across the thylakoid membrane in Arabidopsis. *Journal of integrative plant biology* **2016**, *58*, 848-858, doi:10.1111/jipb.12475.
57. Kim, L.J.; Tsuyuki, K.M.; Hu, F.; Park, E.Y.; Zhang, J.; Iraheta, J.G.; Chia, J.C.; Huang, R.; Tucker, A.E.; Clyne, M.; et al. Ferroportin 3 is a dual-targeted mitochondrial/chloroplast iron exporter necessary for iron homeostasis in Arabidopsis. *Plant J* **2021**, *107*, 215-236, doi:10.1111/tpj.15286.

 doi:10.20944/preprints202603.0998.v1

58. Goodin, M.M.; Zaitlin, D.; Naidu, R.A.; Lommel, S.A. Nicotiana benthamiana: its history and future as a model for plant-pathogen interactions. *Mol Plant Microbe Interact* **2008**, *21*, 1015-1026, doi:10.1094/mpmi-21-8-1015.
59. Gandini, C.; Schmidt, S.; Husted, S.; Schneider, A.; Leister, D. The transporter SynPAM71 is located in the plasma membrane and thylakoids, and mediates manganese tolerance in Synechocystis PCC6803. *New Phytologist* **2017**, *215*, doi:10.1111/nph.14526.